South African Journal of Botany 107 (2016) 188–199

Contents lists available at ScienceDirect

South African Journal of Botany

journal homepage: www.elsevier.com/locate/sajb

Vegetation mapping in the St Lucia estuary using very high-resolution multispectral imagery and LiDAR

M. Lück-Vogel [a,c,*], C. Mbolambi [a], K. Rautenbach [b], J. Adams [b], L. van Niekerk [a,b]

[a] Council for Scientific and Industrial Research, P.O. Box 320, 7599 Stellenbosch, South Africa
[b] Department of Botany, Nelson Mandela Metropolitan University, Summerstrand Campus, 6031 Port Elizabeth, South Africa
[c] Department of Geography and Environmental Studies, Stellenbosch University, 7600 Stellenbosch, South Africa

ARTICLE INFO

Article history:
Received 23 November 2015
Received in revised form 8 April 2016
Accepted 14 April 2016
Available online 5 May 2016

Edited by T Riddin

Keywords:
St Lucia
Estuary
Remote sensing
WorldView-2
RapidEye
SPOT-6

ABSTRACT

This paper examines the value of very high-resolution multispectral satellite imagery and LiDAR-derived digital elevation information for classifying estuarine vegetation types. Satellite images used are from the WorldView-2, RapidEye, and SPOT-6 sensors in 2 m and 5 m resolution, respectively, acquired between 2010 and 2014. Ground truthing reference is a GIS-derived vegetation map based on field data from 2008. Supervised maximum likelihood classification produced satisfactory overall accuracies between 64.3% and 77.9% for the SPOT-6 and the WorldView-2 image, respectively, while the RapidEye-based classifications produced overall accuracies between 55.0% and 66.8%. The reasons for the misclassifications are mainly based on the highly dynamic environmental conditions causing discrepancies between the field data and satellite acquisition dates rather than technical issues. Dynamics in water levels and salinity caused rapid change in vegetation communities. Further, weather impacts such as floods and wind events caused water turbidity and led to bias in the reflective properties of the satellite images and thus misclassifications. These results show, however, that the spatial and spectral resolution of modern very high-resolution imagery is sufficient to satisfactory map estuarine vegetation and to monitor small-scale change. They emphasise, however, the importance of synchronisation of ground truthing data with actual image acquisition dates in these highly dynamic environments in order to achieve high classification accuracies. The results also highlight the importance of ancillary data for accurate interpretation of observed classification discrepancies and vegetation dynamics.

1. Introduction

The St Lucia Estuary is part of the uMfolozi/uMsunduzi/St Lucia estuarine system which forms the largest fluvial coastal plain in South Africa (Van Heerden, 2011) and the largest estuarine system in Africa (155,000 ha). As part of the iSimangaliso Wetland Park, it hosts the highest biodiversity of wetland habitat types for its size in the whole of southern Africa (Cowan, 1999). Besides its tremendous value for biodiversity and nature conservation, this estuarine system also provides the basis for the regional economy such as commercial (sugarcane) crop production, subsistence agriculture, mining, tourism, commercial and subsistence forestry (GTI, 2010). While each of these activities benefits from the ecosystem services of the estuarine systems, they also impact on the condition of the ecosystem in a combined cumulative way.

The presence, abundance, and condition of macrophytes, i.e. higher plants, can be used as indicators to determine the health of estuarine ecosystems (EPA, 2013). However, the paucity of spatial–temporal information on estuarine vegetation composition and distribution in South Africa currently undermines a holistic understanding of estuarine processes and functioning and subsequently the prediction of impacts of major environmental changes. Mapping of the estuarine vegetation would provide a baseline for understanding and monitoring of estuarine biological processes. Remote sensing is widely viewed as an effective way to spatially continuous inventories of vegetation composition, distribution, and condition, in particular in large and inaccessible areas in many regions of the world.

However, in coastal and estuarine environments, the very small scale of the habitats, frequently occurring in narrow bands along the shore, prohibited the application of remote sensing until recently, as most of the satellite images successfully used in other environments did not provide enough spatial detail. Examples are the Landsat 4 to 8 series and the MODIS and NOAA AVHRR sensors.

High and medium resolution data, namely, aerial photographs, SPOT 3, and Landsat TM imagery have been compared by Harvey and Hill (2001) in the Northern Territory, Australia, to determine the accuracy and applicability of each data source for the detailed spectral discrimination of vegetation types in a tropical wetland. They found that aerial photos with a very high spatial resolution provided better classification accuracies than the SPOT and Landsat TM imagery. In accordance with this, Yang (2007) classified riparian vegetation in Australia with an

* Corresponding author.
E-mail address: mluckvogel@csir.co.za (M. Lück-Vogel).

http://dx.doi.org/10.1016/j.sajb.2016.04.010

accuracy of 81% using aerial photos, 63% using SPOT-4 imagery (10 m resolution), and 53% using Landsat 7 imagery (30 m resolution). He pointed out that the low number of spectral bands is the limiting factor in using aerial photos for wetland vegetation classification, as is the coarse spatial resolution in the case of the Landsat imagery.

Only with the recent availability of very high-resolution (VHR) imagery e.g. from the SPOT-6, RapidEye, and Worldview-2 sensors which provide multispectral imagery with pixel sizes between 2 and 5 m and more spectral bands, satellite remote sensing of estuarine and coastal regions has become more feasible. In addition, topographic information derived from airborne LiDAR (Light Detection and Ranging) technology has proven to improve coastal vegetation mapping significantly, in particular when used in combination with multispectral imagery (Prisloe et al., 2006; Kempeneers et al., 2009).

The aim of this paper was therefore to test and compare the use of VHR SPOT-6, RapidEye, and WorldView-2 (WV2) satellite imagery with and without combination of LiDAR data for mapping relevant vegetation types in the St Lucia Estuary.

Fig. 1. The St Lucia system including its lakes and feeder rivers (source: Whitfield, 1992).

The classes that were mapped were aligned with existing habitat keys from the National Biodiversity Assessment (Turpie et al., 2012; Van Niekerk and Turpie, 2012). The intention was to provide guidance on which sensor or sensor combination provides the most accurate spatial information for informing estuarine management. Furthermore, the influence of environmental factors such as wind speed and water levels on the accuracy of the results was examined.

2. Study area

With an area of about 30,520 ha, St Lucia is the largest estuary in South Africa (Moll et al., 1971; Turpie et al., 2012). The climate is subtropical with an average annual rainfall of approximately 1100 mm with most rainfall occurring in winter and spring, i.e. June to October (Taylor et al., 2006). The average temperatures range between 25 and 28 °C throughout the year.

In the south, the estuary mouth is connected to the Indian Ocean by the 21 km long Narrows channel. The lake system is separated from the sea by high coastal dunes that flank its eastern bank (Taylor, 2006), see Fig. 1.

St Lucia has an inlet/mouth that is periodically closed to the sea for months to years at a time depending on the river inflow regime and management interventions. This means that water levels and salinity can change drastically within short periods, e.g. after floods and mouth breaks. In response, the distribution of estuarine vegetation communities is highly dynamic.

The predominant natural estuarine vegetation in the region can be divided into 8 habitat units, namely, permanently flooded macroalgae and submerged macrophytes, partly flooded reeds and sedges and salt marshes, mangroves and swamp forests, and grass and shrub vegetation, and lastly floating macrophytes (Rautenbach, 2015). Table 1 below summarises the dominant species and gives a brief description of these habitat types.

Land use in the vicinity of the estuarine system is diverse. It includes commercial (sugarcane) crop production, subsistence agriculture, mining, tourism, commercial and subsistence forestry, conservation as well as residential areas (GTI, 2010).

The land use in the immediate iSimangaliso Wetland Park (former Greater St Lucia Wetland Park) area changed dramatically during the last two decades. Before the declaration of the Wetland Park as UNESCO World Heritage Site in 1999 (UNESCO, 1999), large areas were used for commercial forestry, introducing alien Eucalypt and Pine species. Since the foundation of the Wetland Park, forestry has been actively removed, and international eco-tourism is becoming more important. In the abandoned forestry areas, a quick succession of natural vegetation can be observed. However, an expansion of rural settlements into the area due to an increase in population (e.g. immigration from Mozambique and other areas), puts a new pressure on natural environments.

3. Material and methods

3.1. Input data

3.1.1. Reference habitat map

As reference map for this study, an existing GIS map based on aerial imagery from 2008 was used. The map only delineates habitats below the 5 m contour. This map was originally generated by Nondoda (2012). A modified version of this map as presented by Rautenbach (2015) which aggregates some of Nondoda's original classes was used for this study. Accuracy and spatial detail was considered suitable for our purpose. The habitat units derived from this data set are Submerged macrophytes, Salt marsh, Swamp forest, Grass and shrubs, Mangroves, and Reeds and Sedges (see Table 1 above).

Table 1
Habitat units and their dominant species (Rautenbach, 2015).

Habitat unit	Dominant species	Description
Macroalgae	*Ulva intestinalis*, *Chaetomorpha* sp., *Cladophora* sp., *Bostrychia* sp. and *Polysiphonia* sp.	Found at estuary margins, as epiphytes and associated with mangrove pneumatophores.
Submerged macrophytes	*Ruppia cirrhosa*, *Zostera capensis* and *Stuckenia pectinata*	Plants rooted in substrata whose leaves and stems are completely submersed.
Reeds and sedges	*Phragmites australis*, *Juncus kraussii* and *Schoenoplectus scirpoides*	Observed at sites with freshwater input at the margins, rooted in submerged substrata. *Juncus kraussii* is observed at the vicinity of the Forks and the Narrows.
Mangroves	*Avicennia marina* and *Bruguiera gymnorrhiza*	Observed in the brackish to saline intertidal areas at the Narrows and mouth area.
Grass and shrubs	*Sporobolus virginicus*, *Paspalum vaginatum*, and *Stenotaphrum secundatum*	Sedge grass and shore slope lawn, observed in areas where there is no freshwater input, freshwater is provided by rainfall.
Salt marsh	*Sarcocornia* sp., *Salicornia meyeriana*, and *Atriplex patula*	Succulent species colonize exposed saline soils in False Bay and in the mudflats of North Lake and are not tolerant to long periods of inundation.
Swamp forest	*Ficus trichopoda*, *Barringtonia racemosa*, and *Voacanga* sp.	Observed on the banks of Mfolozi Estuary, in the vicinity of the back channel and Narrows and along the Eastern Shores under freshwater conditions.
Floating macrophytes	*Nymphaea nouchal*, *Azolla filiculoides*	Floating leaved species are commonly associated with submerged and deepwater aquatics and occur at water depths from 0.5 to 2 m.

3.1.2. LiDAR data

A LiDAR data set acquired in April–May 2013 covering the iSimangaliso Wetland Park area was made available for this project by the iSimangaliso Wetland Park authority. The Digital Terrain Model (DTM) data consisted of high accuracy (1 Sigma) point data of LiDAR-derived surface information, which has been provided in xyz ASCII format as well as in 0.25 m contours in SHP file format. The ASCII format contains very detailed surface information. However, files tend to be huge and require special software to access. In contrast, the SHP format is a format that most GIS practitioners can readily use and it is therefore a common LiDAR output product format. However, the generalisation of the information to derive 25 cm contours means a loss of detail. In order to assess the impact of this loss of detail on the habitat classification accuracy, in this project both the SHP file contour product and the raw, unthinned xyz point cloud data binned to 1 m were used as separate inputs for the habitat classification.

3.1.3. Satellite imagery

For this project, a series of high-resolution satellite images from the RapidEye, SPOT-6, and WorldView-2 sensors was acquired. All imagery was provided in full band mode, geometrically but not radiometrically corrected (level 2B). Table 2 below gives an overview of the respective sensors, the spatial resolution and the respective acquisition dates. The respective spectral bands are given in Table 3 below.

3.2. Areas used for application of approach

For the supervised classification approach, only subsets of the total satellite coverage were used which corresponded largely with the extent of the Wetland Park and the extent of the reference habitat map. In this way, land cover and habitat classes for which no reference data were available and whose accuracy could not have been assessed (e.g. any agriculture and other transformed areas) were largely excluded. The available RapidEye and SPOT-6 data covered almost the full extent of that area, while for WorldView-2 only for the southern part imagery was available.

Table 2
Satellite data used and their specifications.

Sensor	Resolution (m)	Acquisition dates
WorldView-2	2.0	9 April 2010
RapidEye	5.0	18/20 July 2011 13 January 2012
SPOT6	5.0	8 February 2014
LiDAR	Rasterised to match above	April–May 2013

3.3. Methods

The final goal of comparing habitat classifications derived from different combinations of input data has been achieved following several preprocessing, data conversion, and data generation steps. Fig. 2 gives an overview of the work conducted for the Maximum Likelihood classification. The individual preprocessing, classification, and post-processing steps are unpacked in the following sections.

3.3.1. Preprocessing of remote sensing data

All satellite image files were corrected for radiometric and atmospheric effects to derive top of canopy reflectance values. This correction allowed for better analysis of the spectral signatures in the actual classification approach as described in Section 3.3.4 below.

The RapidEye image for July 2011 was provided as seven individual tiles from two separate acquisition dates (18 and 20 July 2011), the RapidEye image for 13 January 2012 as six individual tiles. Following the atmospheric correction of the individual tiles, all the tiles for July 2011 and all tiles for January 2012 were mosaicked to allow for an easier handling of the data in the subsequent work steps.

Some of the satellite images originally came in UTM projection with WGS84 Datum, while others were provided in Transverse Mercator projection. It was decided to reproject all images to the projection of the 2008 reference data: Transverse Mercator, Central Meridian 33°E, Hartebeesthoek 1994 Datum. In this way, the best possible geographical match of the data sets was achieved. It is important that the images to be classified overlay with high geographic accuracy to the reference data, as spatial misalignments can lead to misclassifications and reduced accuracies (Townshend et al., 1992).

Given the humid, subtropical climate of the area, it was very difficult to get 100% cloud-free satellite images; three out of the four images used had some cloud occurrences. A masking of cloud areas was not conducted as a result of time constraints. However, in order to avoid biases in the classification and accuracy results, care was taken in the selection of cloud-free training and validation points instead (Sections 3.3.2 and 3.3.3).

The LiDAR data for that area were provided in individual small tiles as well. Therefore, in a first step, those tiles covering the SPOT-6, RapidEye, and WV-2 mosaics were identified.

For those, both, the 25 cm contour SHP files as well as the unthinned xyz ASCII files binned to 1 m resolution, were converted into an ERDAS IMG raster format matching the spatial resolution of the respective multispectral images (2 and 5 m respectively). The raster tiles were then mosaicked and reprojected to match the projection of the multispectral mosaics.

The elevation data ranges were then stretched and the layers were stacked (i.e. attached) to the respective multispectral images (see respective last layers “contour DEM” and “xyz DEM” in Table 3 below).

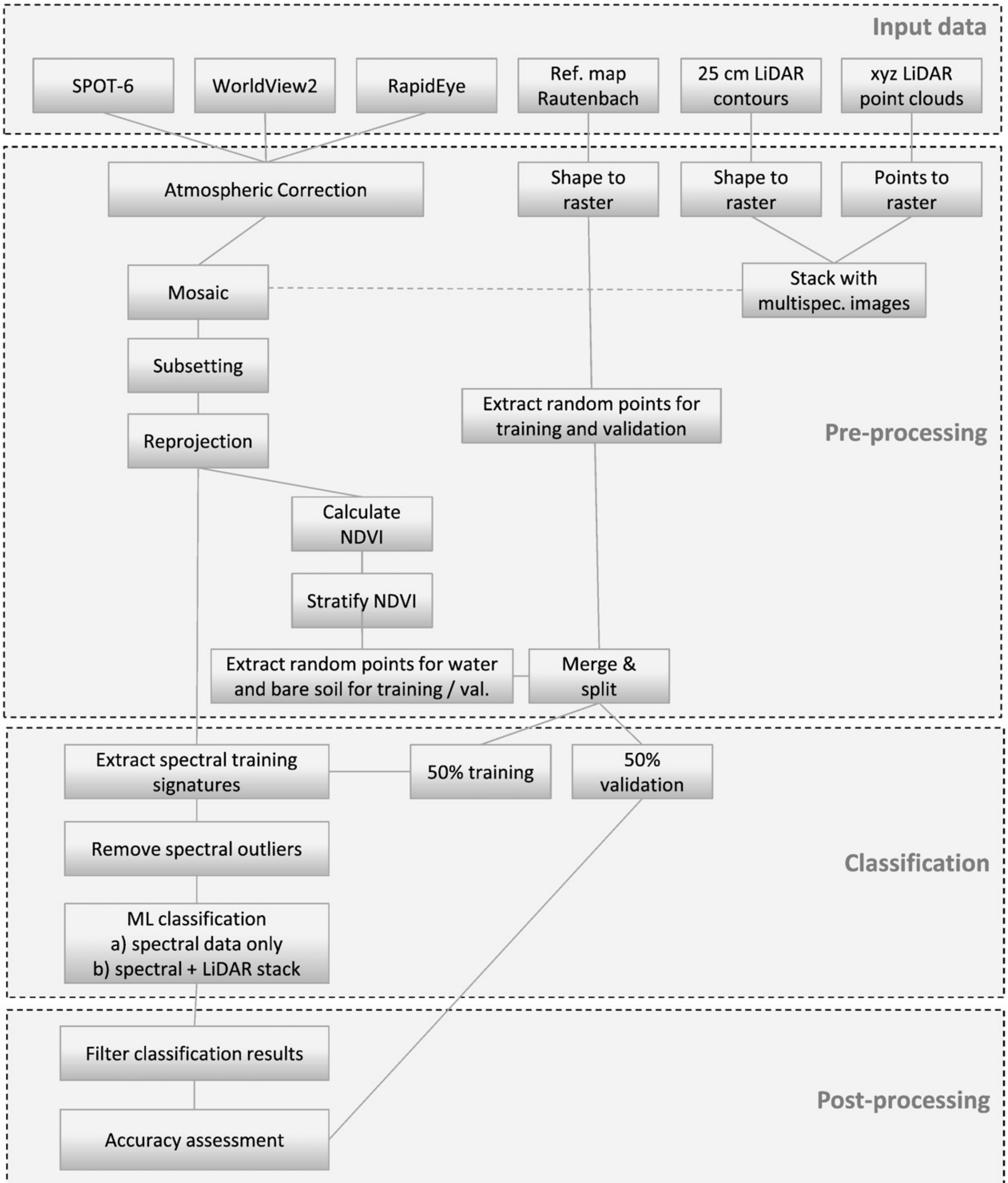

Fig. 2. Flow diagram of technical steps conducted.

The elevation range of the original Terrain model for that area was between −2.5 m and +180 m. This data range is very small when compared to the re-scaled reflectance values of the multispectral images, ranging typically between 500 and 6000. The original small data range of the elevation data would be almost un-noticeable when attached as extra layer to the multispectral image, thus not adding much information for the Maximum Likelihood classification. Therefore, the DEM data were re-scaled using the function [(Image +2.5)*100], leading to a "stretched" data range between 0 and 18,250 which emphasises small variations in relief. Altogether, 8 data stacks were produced as input for the classification process (Table 3).

3.3.2. Extraction of ground truthing points from GIS reference data

The basis for the training and validation data for the classification of the satellite images was the 2008 reference map (Section 3.1.1). For the classes Submerged macrophytes, Salt marsh, Swamp forest, Grass and shrubs, Mangroves, and Reeds and Sedges (Table 1) stratified random points were extracted from that map (Lowry et al., 2007; Duro et al., 2012). Between 20 and 30 points per class per satellite image extent were created. For all resulting points, it was checked visually if any of them was lying in an area impacted by clouds or cloud shadows. Impacted points were omitted to avoid biases in the classification and validation approach.

Table 3
Bands of the respective layer stacks used for the supervised classification process.

Stack no.	1	2	3	4	5	6	7	8
Band no.	WV-2	WV-2	RapidEye 2011	RapidEye 2011	RapidEye 2012	RapidEye 2012	SPOT-6	SPOT-6
1	Coastal	Coastal	Blue	Blue	Blue	Blue	Blue	Blue
2	Blue	Blue	Green	Green	Green	Green	Green	Green
3	Green	Green	Red	Red	Red	Red	Red	Red
4	Yellow	Yellow	RedEdge	RedEdge	RedEdge	RedEdge	NIR	NIR
5	Red	Red	NIR	NIR	NIR	NIR	Contour DEM	xyz DEM
6	RedEdge	RedEdge	Contour DEM	xyz DEM	Contour DEM	xyz DEM		
7	NIR1	NIR1						
8	NIR2	NIR2						
9	Contour DEM	xyz DEM						

3.3.3. Extraction of ground truthing points for Bare soil and Open water

Additional random points for the land cover classes Open water and Bare soil were created, as these classes are highly important in an estuarine and coastal context and it was anticipated that the inclusion of training points for these classes would improve the overall accuracy of the supervised maximum likelihood classification in narrowing the actual feature space for all classes.

For the identification of open water and bare soil area, the normalised Difference Vegetation Index (NDVI) was calculated for all four images, following the formula NDVI = (NIR − Red)/(NIR + Red). The value range for NDVI data is from −1 to +1. It is generally accepted that NDVI values for open water are lower than 0, and values for bare soil are in the positive range just above 0 if images are derived from radiometrically corrected images, as in our case (Loveland et al., 1991; Lunetta et al., 2006). Visual inspection of the actual NDVI data confirmed this rule, only for the RapidEye-derived NDVI data the threshold between water and bare soil had to be adjusted to 0.1 for a visually satisfactory distinction between the two classes.

For Bare soil, an NDVI value range between 0.0 (0.1 for RapidEye) and 0.4 was set. The threshold of 0.4 for delineating bare soil from vegetation appears to be quite high. However, impervious surfaces (i.e. anthropogenic bare surfaces) were characterised by Loveland et al. (1991) by values between 0.3 and 0.4, too. However, for this paper, the threshold has been defined visually from the image, using fallow fields, roads, and the beach as reference. It cannot be excluded though that our class “Bare Soil” would include some sparse vegetation, too.

From the derived Water and Bare Soil masks about 25 random points were extracted for both, training and validation, and added to the respective point sets created from the 2008 habitat reference map. Points impacted by clouds and cloud shadows were removed from these classes as well. For the resulting eight habitat classes, between 154 (WV-2) and 251 (RapidEye) training and validation points, respectively, were used. The variation in point numbers is related to the amount of points which had to be deleted due to cloud and cloud shadow impact. Further, in the 2008 reference map, Salt marsh and Submerged macrophytes did not occur in the southern area covered by the WV-2 image, thus these classes are not represented in the WV-2 classification.

3.3.4. Maximum Likelihood classification

For all four images, spectral training signatures were created for the respective training points for all eight respective layer stacks (Table 3). The resulting spectral signatures were cleaned from obvious outliers that would have contributed to biased spectral statistics in the following classification process. Outliers were caused mainly by changes in land cover in the time between the 2008 reference data and the actual image acquisition date, such as forest plantation to grass and shrubs, or grass and shrubs to swamp forest. Where the analysis of the spectral signatures revealed that there are spectral subgroupings within one of the reference classes, these subclasses were treated as individual classes during the classification process. As an example, the class “Grasses and Shrubs” consisted of areas which were clearly dominated by shrubs, while other areas were dominated by grasses, resulting in either more shrub- or grass-dominated spectral signatures. Here subclasses “Grass and shrubs_woody” and “Grass and shrubs_grassy” were created. Furthermore, some of the reeds were flooded during the time of image acquisition and looked spectrally different from non-flooded reeds. Keeping these spectrally different subgroups of a class separate in the actual classification process has shown to produce higher classification accuracies. The classification process was then run on all 8 layer stacks (as per Table 3) twice, first excluding, then including the contour and xyz DEM, respectively, resulting in a total of 16 classifications.

It was decided to include all multispectral bands of the respective sensors in the classification process to assess the value of the high spectral resolution (i.e. increased number of bands) on the accuracy of the classification results. Schuster et al. (2012) and Adam et al. (2014) emphasise the improvement of land cover classifications by using RapidEye's RedEdge band. For all classifications, Feature Space was selected as the non-parametric rule and Maximum Likelihood as the parametric rule in ERDAS' Supervised classification tool.

3.3.5. Post-processing

Given the high spatial resolution of the satellite images, the 16 classification results looked very “noisy”. This means that the vegetation types were disrupted by single classes or groups of pixels of another class, mainly as a result of shadow effects in the vegetation canopy. It was therefore decided to filter the classification outputs to eliminate those miss-classified single pixels or small pixel groups consisting of <8 pixels (Fig. 3). According to Duro et al. (2012), this smoothing of classification results can improve the overall classification accuracy.

Further, where existing, the interim subclasses (e.g. Sedges and Reeds-flooded and Sedges and Reeds-non-flooded) were merged again to the original class types. This had to be done to have the same level of class detail as the reference habitat map for accuracy assessment purposes.

3.3.6. Accuracy assessment

For all resulting 16 classifications, error matrices including the Overall Accuracy, the User's and Producer's Accuracy for each class, as well as the Kappa coefficient were produced and analysed. The Overall Accuracy gives the percentage of reference points that have been classified correctly. The User's Accuracy indicates the probability that a pixel classified in this class actually represents this class on the ground, and the Producer's Accuracy indicates how accurately the training points have been classified. The Kappa statistic indicates to which extent the classification result is better than pure chance (Lillesand et al., 2004), i.e. the higher the Kappa value, the greater the classification accuracy. The difference between Kappa and Overall Accuracy (OAA) is that the OAA can be biased by differences in the number of reference points per class, i.e. classes with more reference points weigh more in the OAA, while the Kappa is not affect by unequal reference point numbers.

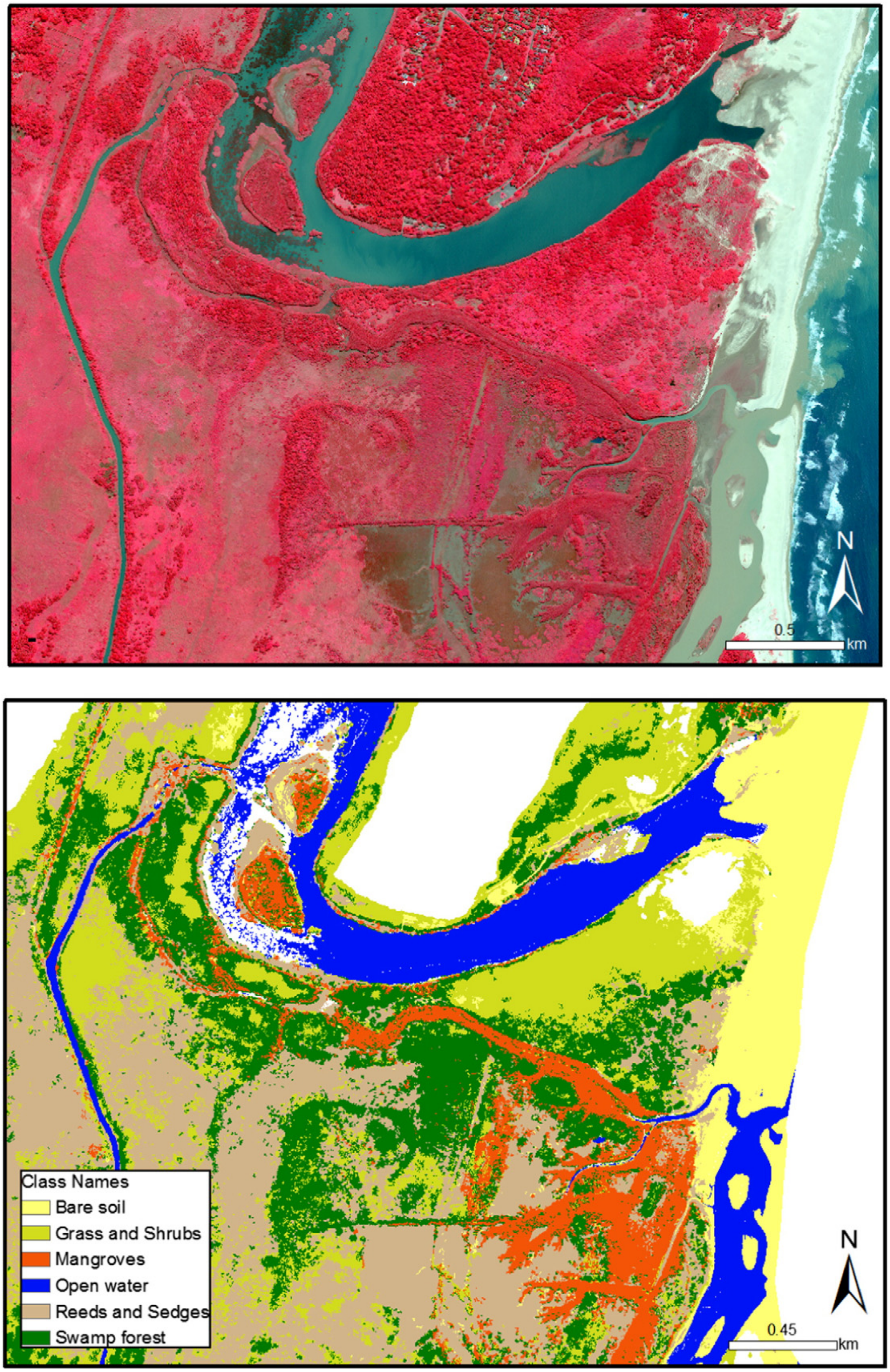

Fig. 3. Example of classification results. Top: Multispectral WV-2 image of the estuary mouth; bottom: final classification results for same area after filtering (areas higher than 10 m above sea level are masked out).

4. Results and discussion

Table 4 below gives an overview of the Overall Accuracies and Kappa values for all 16 (4 × 4) classification runs.

4.1. Impact of LiDAR DEMs on classification accuracies

Comparing runs 1 and 2, and runs 3 and 4 in Table 4 respectively shows that in 7 out of the 8 classifications the additional use of the

Table 4
Overview of Overall Accuracies (OAA) and Kappa values for all classifications.

		2010 WV-2		2011 RapidEye		2012 RapidEye		2014 SPOT-6	
Run no.	DEM type	OAA	Kappa	OAA	Kappa	OAA	Kappa	OAA	Kappa
1	no contours	72.7%	0.66	57.8%	0.52	55.0%	0.48	69.6%	0.64
2	contours	76.6%	0.70	62.5%	0.57	60.2%	0.54	64.3%	0.59
3	no xyz	75.3%	0.69	57.4%	0.51	56.8%	0.50	71.4%	0.67
4	with xyz	77.9%	0.72	66.8%	0.62	57.8%	0.51	75.7%	0.72

LiDAR-derived DEM information improved the overall classification accuracies (OAA). This result is in accordance to other publications, confirming that the combined use of LiDAR and multispectral data improves classification accuracies (e.g. Kempeneers et al., 2009). The LiDAR decreased the accuracy of the classification results in the second run of the SPOT-6 image.

The overall accuracies and Kappas for the purely multispectral-based classifications of the first and third run are about the same for the RapidEye and SPOT-6 images, which was to be expected because in both cases the input is only the multispectral image. However, there is a slight improvement in the third run of the WorldView-2 image, probably caused by slight differences in the respective training areas.

Accuracies for three of the four classifications including the detailed LiDAR information in the fourth run are higher than the respective accuracies for the contour-derived LiDAR stacks in run 2. This indicates that the use of more detailed surface data improves vegetation classification accuracies.

4.2. Confusion between Sedges and Reeds and Grass and Shrubs

Table 5 shows the error matrix for the fourth run of the WorldView-2 classification that included the detailed xyz-derived LiDAR data. This matrix shows how many of the reference data have been classified correctly. For example, of the 19 validation points for Grass and Shrubs (row Ref. Total), 13 have been correctly classified as Grass and Shrubs, but 2 points were classified as Swamp forest and Sedges and Reeds and one as Mangroves and one as Bare soil. Altogether, 33 points have been classified as Grass and Shrubs (Class. Total), 13 of which are in fact Grass and Shrubs, but 9 of the 33 should have been classified as Swamp forest, 1 as Mangroves, and 10 as Sedges and Reeds instead. The last columns give the respective Producer's and User's Accuracy and Kappa value per class.

Table 5 shows that the accuracies for 5 of the 6 classes with Kappas >0.7 are quite high, including the classes Bare soil and Water, which, because of their spectral distinctness from any vegetation classes, in most land cover classifications yield very high accuracies. However, the sensors often confused the classes Grass and Shrubs and Sedges and Reeds, leading to Kappas as low as 0.31 and Accuracies as low as 39.4%. The analysis of the other classifications shows that the same confusion occurred frequently between these two classes.

However, we expect that the high dynamic of the estuarine vegetation, in particular the non-woody classes even over a relatively short observation period of 2 years, would be the main reason for the low accuracy results when measured against the 2008 reference data. High dynamics in the estuarine vegetation have also been reported by Rautenbach (2015) for the period 2008–2013. In other words, our classifications correctly picked up real vegetation changes on the ground.

Further sources for low classification accuracies are:

- *Spectral similarity between the classes*: The more grassy areas of the class Grass and Shrubs might have gotten confused with the also grass-like Sedges and Reeds.
- *Small scale vegetation mosaic*: In case that the vegetation on the ground appears in form of a mosaic of small patches of different vegetation types and that this patchiness had been "generalised" in the 2008 reference map, this might confuse the classification in that either the classifier picked variations up correctly but the generalised reference data did not have the correct resolution, or in the form of spectral mixed pixels, which are "blurry" and do not pick up boundaries between patches correctly.
- *Different water levels*: both vegetation types are bound to sites which are low lying and prone to (and dependent on) various levels of flooding. So even if the vegetation itself did not change between the image date and the reference date, various levels of flooding, spatially and temporally, might have biased the spectral signatures and lead to confusion between these classes. This observation is confirmed by the findings of Fyfe (2003) and Silva et al. (2008) whose wetland classifications were affected by similar effects. Figs. 5 and 6 also illustrate the varying water levels in the area at the time of the satellite observations.
- *Accuracy of the reference data*: The St Lucia wetlands cover a large area, and under various water levels, all sections are not equally accessible (e.g. swampy area with large populations of hippopotami and crocodiles). It stands to reason that in the 2008 reference map, some areas were therefore mapped at a coarser resolution than others. It can therefore not be excluded that those two classes have been confused in that data already.

4.3. Analysis of accuracies of other classes

Fig. 4 below shows the Kappa values for all 8 classes in all 16 classifications. The figure shows that the accuracy for class Submerged macrophytes is consistently high for all three images (class not present in smaller WorldView-2 image extent). This result is in contrast to other findings, e.g. by Adam and Mutanga (2009) who found that submerged

Table 5
Error matrix for the 4th run of the WorldView-2 classification of the stack including the xyz-derived LiDAR information.

Classified data	Sw. forest	G & S	Mangr.	Open water	Bare soil	S & R	Class. Total	Prod. Acc.	Users Acc.	Kappa
Sw. forest	45	2	1	0	0	0	48	81.8%	93.8%	0.90
Gr. & Shrub	9	13	1	0	0	10	33	68.4%	39.4%	0.31
Mangroves	1	1	7	0	0	0	9	70.0%	77.8%	0.76
Open water	0	0	0	22	0	0	22	81.5%	100%	1.00
Bare soil	0	1	1	3	14	0	19	100%	73.7%	0.71
S. & Reeds	0	2	0	0	0	19	21	65.5%	90.5%	0.88
Ref. Total	55	19	10	25	14	29	152			

Overall Classification Accuracy = 77.92%.
Overall Kappa Statistics = 0.723.

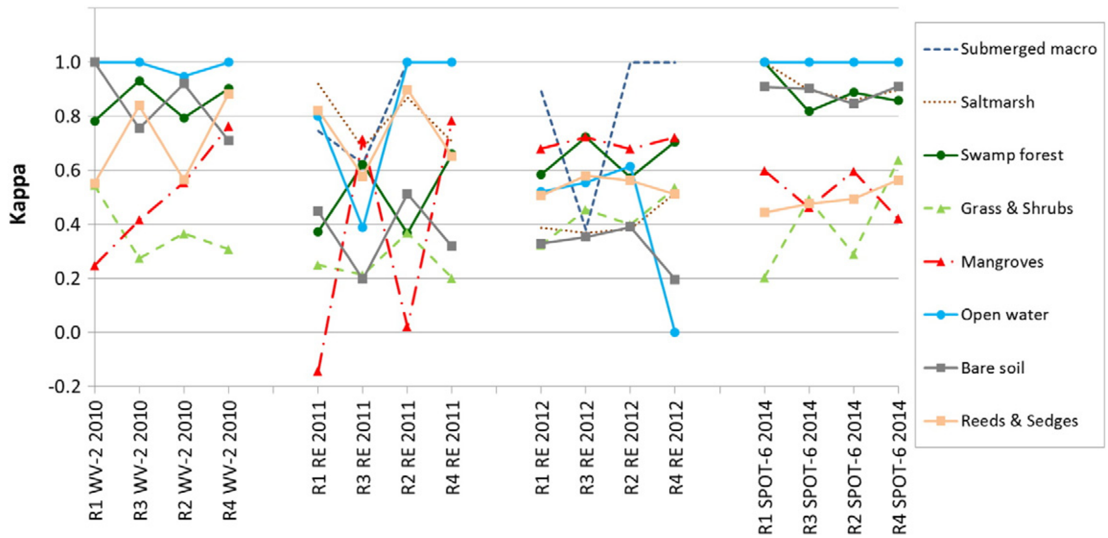

Fig. 4. Kappa values for all classes in all 16 classification runs. R1 and R3: runs without LiDAR DEM, run R2: with contour DEM, run R4: with xyz DEM.

vegetation is difficult to distinguish due to the high water fraction in the spectral signal. Reflectance of water in the infrared band is close to zero, while vegetation has high reflectance in infrared and distinction between species frequently relies on these bands. However, Dogan et al. (2009) used Quickbird data for successful mapping of submerged vegetation as well, which provides 4 spectral bands (visible plus near infrared) in 0.65 m resolution.

Similarly, Swamp forest was consistently mapped with very high accuracies, apart from the DEM-including runs 2 and 4 of the RapidEye images. In contrast, the class Grass and Shrubs frequently was among the lowest accuracies. Mangroves have been classified satisfactory in most of the classifications, too; only in run 1 and run 2 of the 2011 RapidEye image they got confused with Swamp Forest, which means, here the additional use of the DEM increased the separability between the two forest types.

The class Open Water was among the best classes in most of the images, which was expected. Water and Bare soil were classified with very low accuracies, however, in the RapidEye images, and the reasons for this are discussed in Section 4.5 below.

The implication of these results for the user is that Submerged macrophytes, Swamp forest, Mangroves, Open water, and Bare soil are those classes which – according to our results – can be extracted most reliably from the compared WorldView-2, RapidEye, and SPOT-6 images, while the other classes, in particular those with continuously low accuracies, are not so easily distinguishable in an approach as the presented one.

4.4. Comparison of accuracies between sensors

Generally, WorldView-2 produced the best accuracies and SPOT-6 the second best results, while all the RapidEye classifications have strikingly low accuracies (Table 4) with overall accuracies between 55.0 and 66.8% and Kappas as low as 0.48–0.62. The good WV-2 result is expected, given the closest temporal "proximity" to the 2008 reference data. It might be premature though to conclude that WorldView-2 also having the highest spectral and spatial resolution (8 bands, 2 m pixel size) of the compared data sets is the most appropriate for estuarine habitat classification, as, given to the smaller extent of the available image, the total number of classes was lower than in the other images as Submerged macrophytes and Salt marsh did not occur in that area. A lower number of classes usually increases classification accuracies.

SPOT-6 has only 4 spectral bands and a pixel size of 5 m, and with its 10 vegetation classes, it still produced the second best results, which is even more striking, given its largest temporal "distance" from the 2008 reference data. In contrast, both RapidEye images with 5 spectral bands and also 5 m pixel size produced unsatisfactory accuracies for many classes. In comparison, Adam et al. (2014) achieved accuracies above 90% for their RapidEye-based land cover classification in the same region. However, their classes were much broader (bare land, coastal sand, grassland, degraded grassland, indigenous forest, mature sugarcane, young sugarcane, plantation forest, settlements, water body, and wetland) and spectrally more distinct and thus less prone to misclassification than the classes used in this study, where Adam's class "Wetland" actually is divided into six subclasses.

Given the inconsistency of accuracies for individual classes between the compared sensors, in this study, the results are not used for a change analysis of over time, as the results are likely biases by the respective class-related errors.

4.5. Analysis of 2011 and 2012 RapidEye results using environmental condition data

Table 6 shows the error matrix for the 2011 RapidEye classification of the stack including the xyz-derived LiDAR information (run 4) as a typical example for the RapidEye results. Table 7 shows the accuracy matrix for the fourth run of the 2012 RapidEye classification.

In the 2011 result, the class Sedges and Reeds for the reasons described above is confused with Grass and Shrubs. However, in this image, Grass and Shrubs also was confused with Bare soil. It has to be remembered, though, that the Bare Soil mask was produced using an NDVI threshold of 0.4, which is likely to include sparsely vegetated areas as well (compare Section 3.3.3). It is therefore possible that some open Grass and Shrub areas, may be areas recovering after vegetation removal, wrongly fell into the Bare soil class. Further, probably the more woody fraction of the Grass and Shrubs class got confused to a greater extent with the other woody class Swamp forest. Apparently, RapidEye's spectral resolution was not good enough to distinguish between these spectrally similar classes.

Striking, however, is the high degree of confusion and misclassification of the Bare Soil and Water classes in both the 2011 and the 2012 RapidEye images. In most land cover or vegetation classifications, these classes usually produce accuracies of 75%, 80%, or better.

Figs. 5 and 6 might explain the results. At the bottom of Fig. 5 subsets of the Lakes area of the RapidEye and SPOT-6 images are displayed in natural (true) colour. The WorldView-2 image unfortunately did not cover this area. The estuary's water body looks very different in all three images. In the July 2011 image, the water level appears to be moderately high, in the January 2012 image the water level is very low, and in the 2014 SPOT-6 image, the water level appears to be very high. These

Table 6
Error matrix for the 2011 RapidEye classification of the stack including the xyz-derived LiDAR information.

Classified data	Subm.	Salt marsh	Swamp forest	G & S	Mangr.	Open water	Bare soil	S & R	Ref. totals	Prod. Acc.	Users Acc.	Kappa
Submerged	20	0	0	0	0	0	0	0	23	87.0%	100.0%	1.00
Salt marsh	0	20	0	4	0	1	0	2	24	83.3%	74.1%	0.71
Sw. forest	0	0	22	5	1	0	0	3	29	75.9%	71.0%	0.66
Gr. & Shrub	0	2	0	7	3	0	7	6	20	35.0%	28.0%	0.20
Mangroves	0	0	3	0	17	0	0	1	23	73.9%	81.0%	0.79
Open water	0	0	0	0	0	9	0	0	23	39.1%	100.0%	1.00
Bare soil	3	1	0	0	0	13	11	1	18	61.1%	37.9%	0.32
S. & Reeds	0	1	4	4	2	0	0	29	42	69.1%	72.5%	0.65
Col.Total	**23**	**24**	**29**	**20**	**23**	**23**	**18**	**42**	**202**			

Overall Classification Accuracy = 66.83%.
Overall Kappa Statistics = 0.62.

observations are supported by the measured water levels at the St Lucia Bridge (Fig. 6). The water level at the time of acquisition of the 2010 WV-2 image is about the same at the reference time in 2008. The comparable hydrologic conditions with no major water level changes between the two dates resulted in vegetation similarity and contributed to the high accuracies of the WV-2 classification.

The difference in the 2011 and 2012 water levels and the peak water levels in between the reference and image acquisition dates might explain the confusion of the classes which are to be found close to the water edge, as their position will probably have been different from the reference GIS map or vegetation mapped in 2008 might have been washed away during the floods. This result is supported by Rautenbach (2015), who noted: "*The biggest change in vegetation composition* [*between 2008 and 2013*] *was the overall decrease in salt marsh* (*by 57%*) *and increase in submerged macrophytes* (*by 96%*). *After the drought* [*in 2010*], *water level rose rapidly as rainfall returned to normal and the Mfolozi River connected to the sea and St Lucia Estuary. This caused an increase in surface area of the water column* (*which includes the Lakes, Narrows, Back Channel, Link Canal and Mfolozi River*) *from 30 498 ha in 2008 to 32 624 ha in 2013. The increase in water level and the reduction in salinity in False Bay and the lakes* (*North and South*) *caused flooding and inundation of the salt marsh habitat, reducing the area covered.*"

The colour of the water at the image acquisition dates is another potential source for misclassification. In the SPOT-6 image, the water looks relatively clear with only a slight brown discolouration indicating some small degree of turbidity. This may be a result of the mixing of the strong winds 2 days before the image was taken (Fig. 5, top). Given the high water levels at that time, the mixing of the water column would only have been moderate. Flow from the Mfolozi River and entry of water via the back channel and link canal would also result in increased turbidity particularly in the Narrows.

In the 2011 image, however, the water looks greenish, indicating some degree of chlorophyll, either from some microalgae bloom or by submerged macrophyte development. This observation was confirmed by Taylor et al. (2013), who reported high coverages of macrophyte beds in that area which vanished after May 2013. The misclassification of Water as Bare soil (Table 6) supports this observation when considering that our Bare soil based on an NDVI <0.4 likely included some vegetation signal.

In the 2012 RapidEye image, the water looks very turbid and turbulent. Figs. 5 and 6 show that the water level at that time was very low and that during the 3 days preceding the image capture a strong (south-easterly) wind was blowing. Under these conditions, the water column would have been mixed up and very turbid and the water surface very rough with wind-generated waves. (The waves are actually visible when zooming into the image.) This explains the high degree of misclassification between bare soil and water in this image.

5. Conclusions

This paper examined the value of very high-resolution multispectral satellite imagery from the WorldView-2 (2 m pixel size), RapidEye (5 m pixel size), and SPOT-6 (5 m pixel size) sensors acquired between 2010 and 2014 and LiDAR-derived digital surface information for classifying estuarine vegetation types. Ground truthing reference was a GIS-based vegetation map from 2008. Supervised maximum likelihood classification produced satisfactory overall accuracies for the WorldView-2 and the SPOT-6 image, while the RapidEye-based classifications produced slightly lower overall accuracies.

However, the analysis of classification errors in relation to environmental factors showed that mainly high vegetation dynamics, adverse wind conditions, different water levels, and resulting water turbidity seem to be the reason for the observed misclassifications rather than weaknesses of the imagery itself.

It is the inherent dynamic nature of the estuarine environment with large fluctuations in water levels and salinity, which causes swift turnover of vegetation types, temporally and spatially. Examples include

Table 7
Error matrix for the 2012 RapidEye classification of the stack including the xyz-derived DEM information.

Classified data	Subm.	Salt marsh	Swamp forest	G $_amp_$amp; S	Mangr.	Open water	Bare soil	S & R	Ref. totals	Prod. Acc.	Users Acc.	Kappa
Submerged	13	0	0	0	0	0	0	0	18	72.2%	100.0%	1.00
Salt marsh	0	8	0	3	2	0	0	1	26	30.8%	57.1%	0.52
Sw.forest	0	0	26	3	4	0	0	2	29	89.7%	74.3%	0.71
Gr. & Shrub	0	5	1	24	3	0	3	3	40	60.0%	61.5%	0.53
Mangroves	0	0	0	0	12	0	0	4	23	52.2%	75.0%	0.72
Open water	0	0	0	0	0	0	0	0	25	–	–	0.00
Bare soil	5	8	0	2	0	25	16	1	24	66.7%	28.1%	0.20
S. & Reeds	0	5	2	8	2	0	5	34	45	75.6%	60.7%	0.51
Col. Total	18	26	29	40	23	25	24	45	230			

Overall Classification Accuracy = 57.83%.
Overall Kappa Statistics = 0.51.

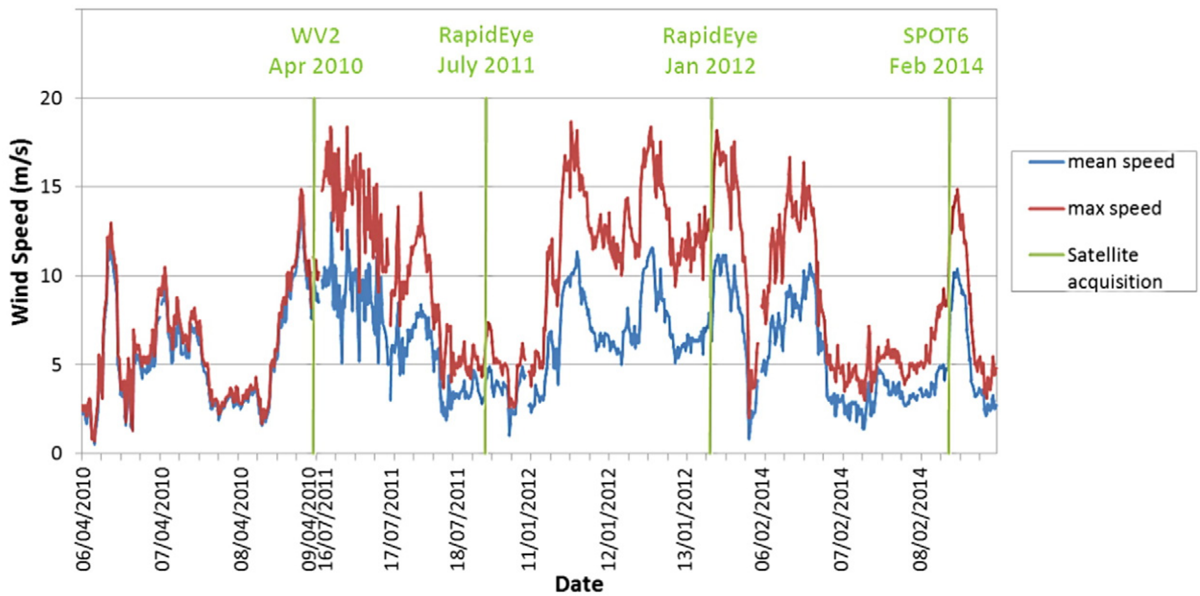

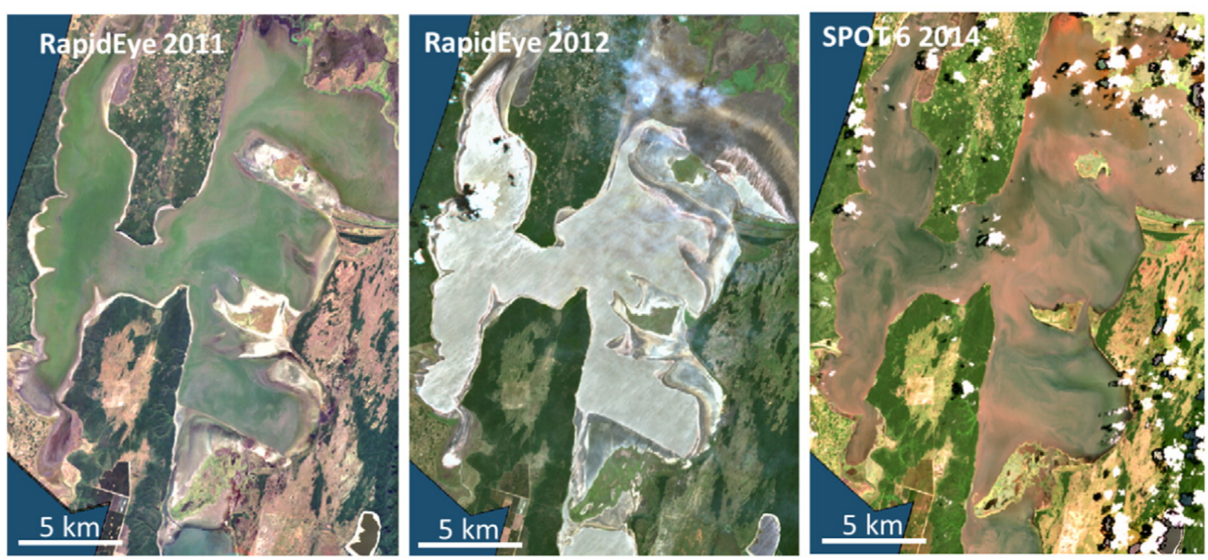

Fig. 5. Top: Hourly wind speed, measured at Richardsbay for 2011–2014 and Durban for 2010 (no Richardsbay data available for 2010), for 3 days prior to respective satellite image acquisition dates. Bottom: Subset of respective RapidEye and SPOT-6 images for the North Lake and False Bay area of the estuary. Wind data source: SADCO (http://sadco.csir.co.za/).

Salt marsh to Sedges and Reeds, or Grass and Shrubs to Swamp forest on abandoned Forest plantations. This leads to inaccurate vegetation classifications if the acquisition date of satellite imagery and the validation data are too far apart. In the St Lucia Estuary, even 6–12 months difference turned out to lead to major vegetation change and hence misclassification, if a major flood eradicated entire vegetation patches or even a recent wind event occurred. It is therefore recommended that ground truthing data are to be used that match the satellite image acquisition dates as closely as possible.

Results were also influenced by physiognomic and spectral similarity of certain vegetation types, such as grass and reeds, and shrubs and forests. This confusion is technically expected. The additional use of LiDAR-derived Digital Surface Models improved the separability of those classes and improved 5 out of 8 classification runs. Further solutions could include either the use of a sensor with a better (hyperspectral) resolution of the satellite imagery or possibly by a more conscious choice of the image acquisition date, where spectral separability varies over the seasons.

Apart from true vegetation change, recent weather impacts (high water levels inundating terrestrial vegetation and wind events mixing up the water column) also contribute to a bias in the reflective properties of the satellite imagery and impair the accurate identification of surface and vegetation types.

Our research showed the importance of ancillary environmental condition data such as water levels, mouth state, wind and weather data to interpret results appropriately. For dynamic environments, such as estuaries and the coast, these data should be sourced routinely as part of any remote-sensing-based vegetation assessment study. This is even more important under (so frequently experienced) project conditions where ground truthing data of the same period are not available.

This research also shows that remote sensing may potentially be more successfully applied to the large permanently open estuaries (~30 of South Africa's systems) as their habitats are more stable than the systems that close with large fluctuations in water levels.

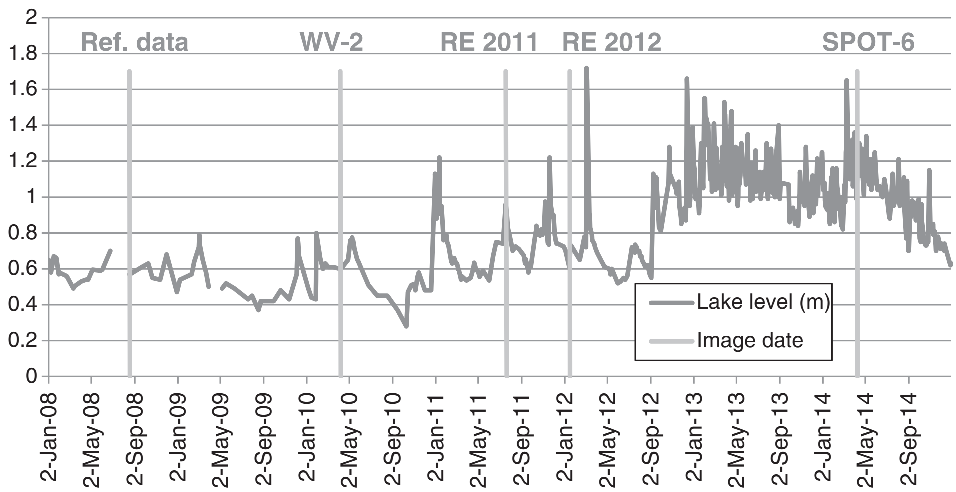

Fig. 6. Water level at the St Lucia Estuary, measured at the St Lucia Bridge (source: Ezemvelo KZN Wildlife). Grey bars: 4× image acquisition dates and 2008 date of reference data collection.

The results show that the spatial and spectral resolution of modern very high-resolution imagery is sufficient to satisfactory map and monitor small-scale estuarine vegetation. They emphasize, however, the importance of synchronisation of ground truthing data with actual image acquisition times in these highly dynamic environments.

6. Acknowledgements

The authors gratefully acknowledge the various sources of funding that enabled the presented research, namely, the GEF (Global Environmental Facility) Project via iSimangaliso Wetland Park Authority for funding Kelly Rautenbach's MSc thesis at the Nelson Mandela Metropolitan University; the Water Research Commission through the research project WRC K5/2268 “Understanding estuarine processes in UMfolozi/Msundazi/St Lucia estuary from earth observation data of vegetation composition, distribution and health” and a Parliamentary Grant to the CSIR's Coastal Systems Research Group for closing loops and writing up. Further to the iSimangaliso Wetland Park for access for field visits, invaluable discussions and access to the LiDAR data of the area that were acquired for its GEF project “Development, Empowerment and Conservation in the iSimangaliso Wetland Park and Surrounding Region Project”. Satellite imagery has been provided by the BlackBridge Company (RapidEye), EADS through the South African National Space Agency (SPOT-6) and DigitalGlobe (WorldView-2).

References

Adam, E., Mutanga, O., 2009. Spectral discrimination of *papyrus* vegetation (*Cyperus papyrus* L.) in swamp wetlands using field spectrometry. ISPRS Journal of Photogrammetry and Remote Sensing 64, 612–620.

Adam, E., Mutanga, O., Odindi, J., Abdel-Rahman, E.M., 2014. Land-use/cover classification in a heterogeneous coastal landscape using RapidEye imagery: evaluating the performance of random forest and support vector machines classifiers. International Journal of Remote Sensing 35, 3440–3458.

Cowan, G.I., 1999. The St Lucia System. (Available online at) http://hdl.handle.net/1834/460 (Last accessed 17 Nov. 2015).

Dogan, O.K., Akyurek, Z., Beklioglu, M., 2009. Identification and mapping of submerged plants in a shallow lake using Quickbird satellite data. Journal of Environmental Management 90, 2138–2143.

Duro, D.C., Franklin, S.E., Dubé, M.G., 2012. A comparison of pixel-based and object-based image analysis with selected machine learning algorithms for the classification of agricultural landscapes using SPOT-5 HRG imagery. Remote Sensing of Environment 118, 259–272.

EPA, 2013. http://water.epa.gov/scitech/swguidance/standards/criteria/aqlife/biocriteria/index.cfm (Last accessed 17 Nov. 2015).

Fyfe, S.K., 2003. Spatial and temporal variation in spectral reflectance: are seagrasses spectrally distinct? Limnology and Oceanography 48, 464–479.

GTI, 2010. 2008 KZN province land-cover mapping (from SPOT 5 Satellite imagery ca. 2008) – data users report and meta data (version 1.0). Published by GeoTerraImage GTI (Pty) Ltd, South Africa, for Ezemvelo KZN Wildlife (Biodiversity Research) (October 2010).

Harvey, K.R., Hill, J.E., 2001. Vegetation mapping of a tropical freshwater swamp in the Northern Territory, Australia: a comparison of aerial photography, Landsat TM and SPOT satellite imagery. Remote Sensing of Environment 22, 2911–2925.

Kempeneers, P., Deronde, B., Provoost, S., Houthuys, R., 2009. Synergy of airborne digital camera and Lidar data to map coastal dune vegetation. Journal of Coastal Research 53, 73–82.

Lillesand, T.M., Kiefer, R.W., Chipman, J.W., 2004. Remote Sensing and Image Interpretation. fifth ed. John Wiley & Sons, New York.

Loveland, T.R., Merchant, J.W., Ohlen, D.O., Brown, J.F., 1991. Development of a Land-Cover Characteristics Database for the Conterminous U.S. Photogrammetric Engineering & Remote Sensing 57, 1453–1463.

Lowry, J., Ramsey, R.D., Thomas, K., Schrupp, D., Sajwaj, T., Kirby, J., Waller, E., Schrader, S., Falzarano, S., Langs, L., Manis, G., Wallace, C., Schulz, K., Comer, P., Pohs, K., Rieth, W., Velasquez, C., Wolk, B., Kepner, W., Boykin, K., O'Brien, L., Bradford, D., Thompson, B., Prior-Magee, J., 2007. Mapping Moderate-Scale Land-Cover over Very Large Geographic Areas within a Collaborative Framework: A Case Study of the Southwest Regional Gap Analysis Project (SWReGAP). Remote Sensing of Environment 108, 59–73.

Lunetta, R.S., Knight, J.F., Ediriwickrema, J., Lyon, J.G., Worthy, L.D., 2006. Land-cover change detection using multi-temporal MODIS NDVI data. Remote Sensing of Environment 105, 142–154.

Moll, E.J., Ward, C.J., Steinke, T.D., Cooper, K.H., 1971. Our mangroves threatened. African Wildlife 26, 103–107.

Nondoda, S.P., 2012. Macrophyte distribution and responses to drought in the St. Lucia Estuary MSc. thesis Nelson Mandela Metropolitan University (NMMU), South Africa.

Prisloe, S., Wilson, M., Civco, D., Hurd, J., Gilmore, M., 2006. Use of Lidar data to aid in discriminating and mapping plant communities in tidal marshes of the lower Connecticut River: preliminary results. Annual Conference of the American Society for Photogrammetry and Remote Sensing. Presented at the Prospecting for Geospatial Information Integration. American Society for Photogrammetry and Remote Sensing, Nevada (ftp://jetty.ecn.purdue.edu/jshan/proceedings/asprs2006/files/0119.pdf, Last accessed 17 Nov. 2015).

Rautenbach, K., 2015. Present State of Macrophytes and Responses to Management Scenarios at the St. Lucia and Mfolozi Estuaries MSc thesis Nelson Mandela Metropolitan University (NMMU), South Africa.

Schuster, C., Förster, M., Kleinschmit, B., 2012. Testing the red edge channel for improving land-use classifications based on high-resolution multi-spectral satellite data. International Journal of Remote Sensing 33, 5583–5599.

Silva, T.S.F., Costa, M.P.F., Melack, J.M., Novo, E., 2008. Remote sensing of aquatic vegetation: theory and applications. Environmental Monitoring and Assessment 140, 131–145.

Taylor, R.H., 2006. Ecological Responses to Changes in the Physical Environment of the St. Lucia Estuary PhD Thesis Norwegian University of Life Sciences (Papers 1, 2 and 3).

Taylor, R., Adams, J.B., Haldorsen, S., 2006. Primary habitats of the St Lucia Estuarine System, South Africa, and their responses to mouth management. African Journal of Aquatic Science 31, 31–41.

Taylor, R., Fox, C., Mfeka, S., 2013. Monitoring the St Lucia Estuarine System: A Synthesis and Interpretation of the Monitoring Data for May 2013. Unpublished Ezemvelo KZN Wildlife report. (16 pages).

Townshend, J.R.G., Justice, C.O., Gurney, C., McManus, J., 1992. The impact of misregistration on change detection. IEEE Transactions on Geoscience and Remote Sensing 30, 1054–1060.

Turpie, J.K., Wilson, G., Van Niekerk, L., 2012. National Biodiversity Assessment 2011: National Estuary Biodiversity Plan for South Africa – Technical Report. Anchor Environmental Consultants Report No. AEC2012/01, Cape Town.

UNESCO, 1999. UNESCO World Heritage Committee, Report of the 23rd Session, Marrakesh, Morocco, 29 Nov- 4 Dec 1999. WHC Report No. WHC-99/CONNF.209/22, Paris, March 2000 (Available online at http://whc.unesco.org/archive/1999/whc-99-conf209-22e.pdf. Last accessed 17 Nov. 2015).
Van Heerden, I.L., 2011. Management concepts for the Mfolozi flats and estuary as a component of the management of the iSimangaliso Wetland Park. In: Bate, G.C., Whitfield, A.K., Forbes, A.T. (Eds.), A Review of Studies on the Mfolozi Estuary and Associated Flood Plain, with Emphasis on Information Required by Management for Future Reconnection of the River to the St Lucia System. Report to the Water Research Commission. WRC Report No. KV 255/10. WRC, Pretoria.
Van Niekerk, L., Turpie, J.K. (Eds.), 2012. South African National Biodiversity Assessment 2011: Technical Report. Volume 3: Estuary Component. CSIR Report Number CSIR/NRE/ECOS/ER/2011/0045/B. Council for Scientific and Industrial Research, Stellenbosch.
Whitfield, A.K., 1992. A characterization of Southern African Estuarine Systems. Southern African Journal of Aquatic Sciences 18, 89–103.
Yang, X., 2007. Integrated use of remote sensing and geographic information systems in riparian vegetation delineation and mapping. International Journal of Remote Sensing 28, 353–370.